文章编号: 1001-9014(2018)06-0653-04　　DOI:10.11972/j.issn.1001-9014.2018.06.002

A simple approach to obtain 2.0 μm GaSb laser by using high-order distributed Bragg reflector

HUANG Shu-Shan[1,2], YANG Cheng-Ao[1,2], ZHANG Yu[1,2*], XIE Sheng-wen[1,2], LIAO Yong-Ping[1,2], CHAI Xiao-Li[1,2], XU Ying-Qiang[1,2], NIU Zhi-Chuan[1,2]

(1. State Key Laboratory of Superlattices and Microstructures, Institute of Semiconductors, Chinese Academy of Sciences, Beijing 100083, China;
2. College of Materials Science and Opto-Electronic Technology, University of Chinese Academy of Sciences, Beijing 100049, China)

Abstract: GaSb-based DBR lasers with high-order Bragg gratings are fabricated without complex process. The 16^{th}-order and 24^{th}-order Bragg gratings are fabricated with double-trench ridge waveguide by using standard contact optical lithography respectively. The 16^{th}-order Bragg grating laser achieves single longitudinal mode continuous-wave (CW) operation at room temperature with side mode suppression ratio (SMSR) as high as 17.5 dB. The maximum single mode continuous-wave output power is more than 10 mW at room temperature. The laser shows a very excellent wavelength stability against injection current. The single spatial mode operation is maintained in the entire injection current range. The 24^{th}-order Bragg grating laser even shows a side mode suppression ratio up to 22.5 dB at room temperature. The emission wavelength is around 2.0 μm.

Key words: laser diodes, quantum well, infrared
PACS: 42.55.Px, 78.55.Cr, 78.67.De

利用高阶DBR实现简单的2.0 μm GaSb激光器

黄书山[1,2], 杨成奥[1,2], 张　宇[1,2*], 谢圣文[1,2], 廖永平[1,2], 柴小力[1,2], 徐应强[1,2], 牛智川[1,2]
(1. 中国科学院半导体研究所 超晶格与微结构国家重点实验室,北京　100083;
2. 中国科学院大学 材料科学与光电技术学院,北京　100049)

摘要:利用高阶Bragg光栅成功制备出GaSb基DBR激光器,避免了复杂的制备工艺.利用标准接触曝光制备出16阶和24阶Bragg光栅以及双沟脊条波导结构.16阶Bragg光栅器件在室温下实现了SMSR高达17.5 dB的单模激光输出.CW状态下室温最大单模输出功率超过10 mW.随着注入电流变化,器件表现出出色的波长稳定性.在整个注入电流范围内,器件都保持单横模工作状态.24阶Bragg光栅器件室温SMSR为22.5 dB.器件的激射波长都在2.0 μm左右.

关　键　词:激光二极管;量子阱;红外

中图分类号:TN2　　**文献标识码**:A

Introduction

Semiconductor laser diodes emitting wavelength around 2.0 μm are attracting more and more attention recently due to a wide variety of applications ranging from remote gas sensing, free-space communication, medical and defense applications[1-5]. Currently the research of semiconductor laser is mainly based on GaAs and InP substrates. The processing methods for these materials are well-developed. Unfortunately, the emission wavelength range around 2.0 μm is difficult to obtain from these materials[6]. However, a variety of molecules such as CH_4 and CO_2 have strong absorption lines in this wavelength region, making the lasers emitting at 2.0 μm wavelength region very important for atmospheric green-

Received date: 2018-02-12, **revised date**: 2018-08-24　　**收稿日期**:2018-02-12, **修回日期**:2018-08-24
Foundation items: Supported by National Basic Research Program of China (2014CB643903), National Natural Science Foundation of China (61790581, 61435012)
Biography: HUANG Shu-Shan (1993-), male, Beijing, China, Ph. D. Research area involves GaSb laser diodes. E-mail: shshuang@semi.ac.cn
* **Corresponding author**: E-mail: zhangyu@semi.ac.cn

house gas sensing[7]. Thus, GaSb-based lasers which can be realized with emission wavelengths above 1.8 μm for room temperature operation draw more and more interest. The recent research works of GaSb laser focus mainly on expanding the wavelength[8-10], increasing the output power and efficiency[1,5] or optimizing the modal quality[11-12]. Moreover, Zhuo Deng *et al*. have investigated the effects of p-type beryllium (Be) doping on the optical properties of GaSb epilayers recently. Their research results suggest an improved optical quality in the Be-doped GaSb layer[13]. The electrical properties have been further studied as well. V. H. Compeán-Jasso *et al*. have demonstrated a very high abrupt breakdown voltage as high as 38 V of the p-GaInAsSb/n-GaSb junction[14]. These results of the GaSb laser demonstrate a significant superiority among many choice to obtain 2.0 μm emission, benefiting from their low cost, small size and excellent laser properties.

As for accurate gas sensing, the lasers must have narrow spectral linewidth, good beam quality and moderate tuning range, meaning that the lasers must attain single longitudinal and spatial mode operation[6]. To limit the operation of the device to a fundamental spatial mode, narrow ridge waveguide defined by a small effective refractive index step Δn is widely employed. As for single longitudinal mode operation, the distributed Bragg reflector (DBR) is widely used. But there is a very great challenge due to the difficulty of device fabricating process, especially DBR fabricating. Several different approaches can be used for making Bragg gratings, such as e-beam lithography (EBL)[15], interference lithography[16-17], and nanoimprint lithography[4,6]. EBL is expensive and inefficient, leading costly and time consuming. Although interference lithography and nanoimprint lithography are good at defining Bragg gratings on surface, making the high aspect ratio etching challenging. All of them have different disadvantages among cost, efficiency, or process[17]. And some of them must divide the fabrication of Bragg grating and ridge waveguide into two steps, making the process more complex. Thus, we want to find a simple path to obtain single longitudinal operation, which makes use of high-order Bragg grating to relax the fabrication process.

In this letter, we report high-order DBR lasers whose Bragg gratings and ridge waveguide are patterned in one step, utilizing standard contact optical lithography in combination with inductively coupled plasma (ICP) etching techniques. This makes the fabricating process predigest significantly. The GaSb-based DBR lasers are manufactured with two different order Bragg gratings. Both of them show good single longitudinal and spatial mode performance around 2.0 μm.

1 Device design and fabrication

The laser structure was grown on a (100) oriented n-type GaSb substrate via solid source molecular beam epitaxy (MBE). The laser structure contains a GaSb buffer layer followed by a 2.0 μm-thick $Al_{0.5}Ga_{0.5}As_{0.02}Sb_{0.98}$ n-type bottom cladding layer. The undoped active structure for a wavelength around 2.0 μm consists of a 10-nm-thick single $In_{0.2}Ga_{0.8}Sb$ quantum well embedded in two 270-nm-thick $Al_{0.25}Ga_{0.75}As_{0.02}Sb_{0.98}$ waveguide layers. The p-type top cladding layer is composed of 2.0 μm-thick $Al_{0.5}Ga_{0.5}As_{0.02}Sb_{0.98}$ layer. The entire structure ended with a 250-nm-thick heavily p-doped (1×10^{19} cm^{-3}) GaSb contact layer to attain a good ohm contact.

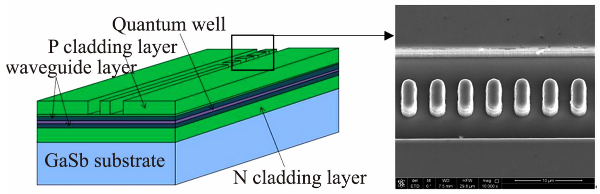

Fig. 1 Schematic layout of the DBR laser device. Inset: SEM images of DBR grating

图 1 DBR 激光器的示意图. 插图:光栅的 SEM 图像

To verify the tentative performance of high-order DBR lasers, preliminary devices were processed into double-trench ridge waveguide. A 5-um-wide and 1 500 μm-long ridge waveguide was designed for single spatial mode operation. The 16^{th}-order Bragg gratings have a period of 4 210 nm and a grating teeth width of 2 105 nm, forming a grating duty cycle of 50%. We manufactured the 16^{th}-order Bragg grating and ridge by standard contact optical lithography simultaneously, decreasing the DBR device fabricating complexity greatly. After the MBE growth, a 400-nm-thick SiO_2 was first deposited on the top of the epitaxial wafer by utilizing plasma enhanced chemical vapor deposition (PECVD) as etching protecting mask during the etching. Taking use of the hard mask and photoresist together instead of photoresist only makes the grating have steep section and stay the stable size of the pattern. The wafer was then spin-coated with photoresist. Then the grating and ridge were patterned on SiO_2 layer using contact lithography and inductively coupled plasma (ICP) dry etching. The pattern transformed from SiO_2 layer to epilayer using ICP dry etching, SiO_2 layer working as hard mask. ICP was used for the second time to clean the residual SiO_2 away. After a new 400-nm-thick SiO_2 layer was deposited by PECVD on the pattern, a current injecting window on the ridge was opened using ICP dry etching. Then we sputtered Ti/Pt/Au as p-side top Ohm contact through using a magnetron sputtering system. The bottom Ohm contacts were formed by utilizing fast-annealed alloyed Au/Ge/Ni/Au after wafer thinning of GaSb substrate. After that, the devices were mounted epi-side down using indium solder on copper heat sinks.

2 Laser performances

The lasers were characterized after the fabricating process. The power-current-voltage (*L-I-V*) characteristics of the 16^{th}-order DBR device in the CW mode at room temperature are shown in Fig. 2. The voltage remains below 3.5 V, indicating a low series resistance. The curve of output power shows a clear threshold current of 160 mA. Even working at room temperature, an optical output power of more than 14 mW could be obtained for an injection current of 1.1 A.

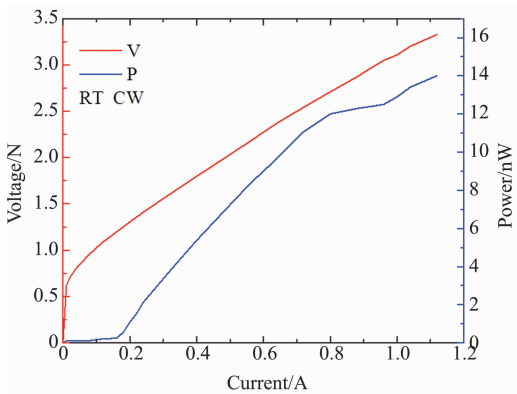

Fig. 2 Power-current-voltage characteristic of a DBR laser at room temperature
图 2 室温下连续模式工作 DBR 激光器的功率—电流—电压特性曲线

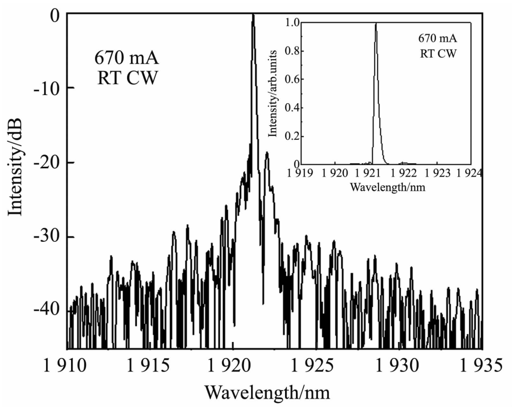

Fig. 3 Representative emission spectrum of a DBR laser with an injection current of 670 mA
图 3 DBR 激光器在注入电流为 670 mA 时的激射光谱

The high-resolution emission spectrum of the 16^{th}-order DBR laser operating with an injection current of 670 mA at room temperature is shown in Fig. 3. The emission wavelength for these conditions is 1 921.2 nm. The laser shows a single longitudinal mode operation with a side mode suppression ratio (SMSR) as high as 17.5 dB, corresponding to approximately 10.3 mW optical output power. As expected, the spectrum shows stabilized emission around the predefined wavelength. The unwanted wavelengths in the gain spectrum of normal Fabry - Pérot laser have been suppressed. Meanwhile, the wavelength which matches the DBR has a significant emission peak in the spectrum, leading single longitudinal mode operation.

The characteristics of emission spectrum and wavelength against current at room temperature are measured. Figure 4 shows the emission spectrum of the laser at each injection current. Figure 5 shows the DBR emission wavelength as a function of the injection current at room temperature. When the injection current increases from 440 mA to 1 040 mA, the emission wavelength shifts from 1 920.4 nm to 1 922.4 nm. The slope is estimated to be

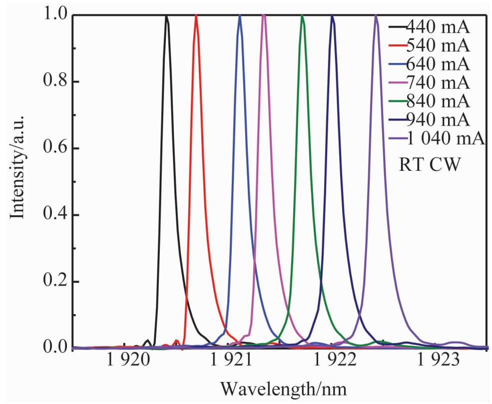

Fig. 4 Emission spectra of a DBR laser at different injection currents
图 4 DBR 激光器在不同注入电流下的激射光谱

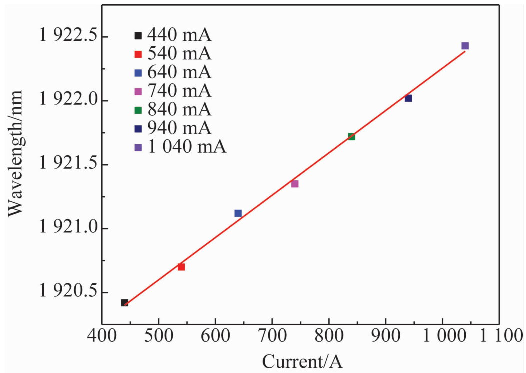

Fig. 5 Emission peak wavelengths of a DBR laser at different injection currents
图 5 DBR 激光器在不同注入电流下的激射波长

about 3.3 nm/A. This slope is most likely determined by the change in effective index of the laser structure. It is much less than that of Fabry - Pérot laser whose emission wavelength more freely fellows the peak in the gain spectrum, showing a typical characteristic of DBR laser to make the wavelength stable.

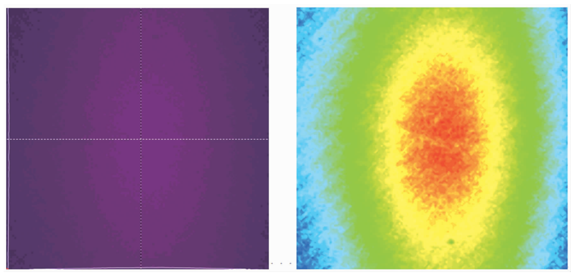

Fig. 6 Far-field images of a DBR laser. Left: measured; right: plotted by using data
图 6 DBR 激光器的远场图像,左边:实际测量的图像;右边:用测量数据画的图像

Measured and plotted far-field images for the DBR laser at injection current of 0.8 A are shown in Fig. 6. The contrast and definition of the measured image are not so clear due to the low optical output power. Thus, we plot the image by using data measured, which is defined as right of Fig. 6. It can be seen that the laser maintains single spatial mode operation.

To demonstrate the capability of DBR lasers using higher order Bragg gratings indeed, DBR lasers with 24^{th}-order gratings were manufactured as the same process mentioned above. The 24^{th}-order Bragg gratings have a period of 6 316 nm and a grating teeth width of 3 158 nm, forming a grating duty cycle of 50%. The representative emission spectrum of the 24^{th}-order DBR laser measured at room temperature is shown in Fig. 7. The emission wavelength is 1 951. 3 nm. The device shows a single longitudinal mode operation with a SMSR as high as 22. 5 dB at an injection current of 860 mA. There is a difference between the 16^{th}-order DBR laser's emission wavelength and that of the 24^{th}-order DBR laser. The difference is probably caused by the wavelength change of the maximum reflectivity for the different Bragg gratings due to the variation of the average effective index determining the Bragg wavelength. Comparing the emission spectra of the different lasers in Fig. 3 and Fig. 7, the peak's width of the 16^{th}-order DBR laser is much less than that of the 24^{th}-order DBR laser. The results show that the wavelength range of high reflectivity for Bragg grating may expand with their order. If the lasers work at the temperature control condition, e. g. 20℃, instead of the room temperature, the SMSR will have a significant increase.

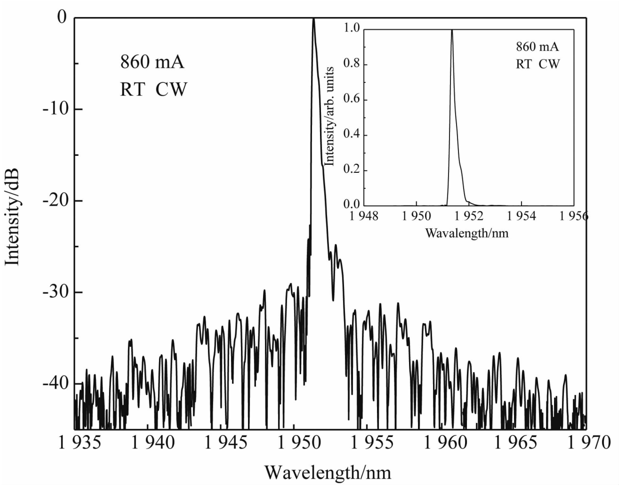

Fig. 7 Emission spectrum of the 24^{th}-order DBR laser at 860 mA

图 7 24 阶 DBR 激光器在 860 mA 时的激射光谱

3 Conclusion

We successfully present a very simple approach to obtain 2.0 μm single longitudinal and spatial mode operation by using high-order distributed Bragg reflector GaSb laser. The 16^{th}-order and 24^{th}-order gratings are patterned by using standard contact optical lithography and ICP with the ridge waveguide simultaneously, reducing the fabricating complexity sharply. The laser operates in a single longitudinal and spatial mode at room temperature with a SMSR as high as 17. 5 dB. The laser's SMSR is even up to 22. 5 dB. The SMSR of the laser still has a very sufficient area to increase with the strict temperature control. The wavelength stability against current shows a typical characteristic of DBR laser. The device emits up to 10 mW at room temperature, giving the device a very significant value in mid-infrared application. The results show the capability of DBR GaSb-based lasers by using high order Bragg gratings as well.

References

[1] Liao Y P, Zhang Y, Yang C A, *et al*. High-power, high-efficient GaSb-based quantum well laser diodes emitting at 2 μm[J]. *J. Infrared Millim. Waves*, 2016, **35**(6): 672-675.

[2] Scholle K, Fuhrberg P, Koopmann P, *et al*. *2 μm laser sources and their possible applications* [M]. Rijeka: INTECH Open Access Publisher, 2010: 437-441.

[3] Xing J L, Zhang Y, Liao Y P, *et al*. Room-temperature operation of 2. 4 μm InGaAsSb/AlGaAsSb quantum-well laser diodes with low-threshold current density[J]. *Chin. Phys. Lett.*, 2014, **31**(5): 054204.

[4] Viheriala J, Haring K, Suomalainen S, *et al*. High spectral purity high-power GaSb-based DFB laser fabricated by nanoimprint lithography[J]. *IEEE Photon. Technol. Lett.*, 2016, **28**(11): 1233-1236.

[5] Liao Y P, Zhang Y, Xing J L, *et al*. High power laser diodes of 2 μm AlGaAsSb/InGaSb type I quantum-wells[J]. *J. Semicond.*, 2015, **36**(5): 054007.

[6] Haring K, Viheriälä J, Viljanen M R, *et al*. 2 μm InGaSb/GaSb laterally coupled distributed feedback laser fabricated by nanoimprint lithography[C]. *In Society of Photo-Optical Instrumentation Engineers. Society of Photo-Optical Instrumentation Engineers (SPIE) Conference Series*, 2010.

[7] Vicet A, Yarekha D A, Pérona A, *et al*. Trace gas detection with antimonide-based quantum-well diode lasers[J]. *Spectrochim.. Acta A*, 2002, **58**(11): 2405-2412.

[8] Chai X L, Zhang Y, Liao Y P, *et al*. High power GaSb-based 2. 6 μm room-temperature laser diodes with InGaAsSb/AlGaAsSb type I quantum-wells[J]. *J. Infrared Millim. Waves*, 2017, **36**(3): 257-260.

[9] Xing J L, Zhang Y, Xu Y Q, *et al*. High quality above 3 μm mid-infrared InGaAsSb/AlGaInAsSb multiple-quantum well grown by molecular beam epitaxy[J]. *Chin Phys B*, 2014, **23**(1): 017805.

[10] Hosoda T, Wang M, Shterengas L, *et al*. Three stage cascade diode lasers generating 500 mW near 3. 2 μm[J]. *Appl. Phys. Lett.*, 2015, **107**(11): 121108-50.

[11] Milde T, Assmann C, Jimenez A, *et al*. Single mode GaSb diode lasers for sensor applications in a long wavelength regime[J]. *Appl Opt*, 2017, **56**(31): H45.

[12] Apiratikul P, He L, Richardson C J K. 2 μm laterally coupled distributed-feedback GaSb-based metamorphic laser grown on a GaAs substrate[J]. *Appl. Phys. Lett*, 2013, **102**(23): 231101.

[13] Deng Z, Chen B, Chen X, *et al*. Optical properties of beryllium-doped GaSb epilayers grown on GaAs substrate[J]. *Infrared Phys. Technol.*, 2018, **90**: 115-121.

[14] Compeán-Jasso V H, de Anda-Salazar F, Sánchez-Niño F, *et al*. High and abrupt breakdown voltage $In_{0.15}Ga_{0.85}As_{0.14}Sb_{0.86}$/GaSb junctions grown by LPE[J]. *Infrared Phys. Technol.*, 2016, **79**: 32-35.

[15] Miller L M, Verdeyen J T, Coleman J J, *et al*. A distributed feedback ridge waveguide quantum well heterostructure laser[J]. *IEEE Photon. Technol. Lett.*, 1991, **3**(1): 6-8.

[16] Li J, Cheng J. Laterally-coupled distributed feedback laser with first-order gratings by interference lithography[J]. *Electron. Lett.*, 2013, **49**(12): 764-765.

[17] Yang C A, Zhang Y, Liao Y P, *et al*. 2 μm single longitudinal mode GaSb-based laterally coupled distributed feedback laser with regrowth-free shallow-etched gratings by interference lithography[J]. *Chin. Phys. B*, 2016, **25**(2): 024204.